

Article

Experimental Research on Dynamic Filtering Characteristics of Filter Materials for Electrostatic-Fabric Integrated Precipitator

Kuixu Chen ^{1,2}, Yaji Huang ^{1,*}, Sheng Wang ³, Zhaoping Zhu ² and Haoqiang Cheng ¹

¹ Key Laboratory of Energy Thermal Conversion and Control of Ministry of Education, School of Energy and Environment, Southeast University, No. 2 Sipailou, Nanjing 210096, China; 13859585878@139.com (K.C.); cheng_phd@163.com (H.C.)

² Fujian Longking Co., Ltd., Longyan 364000, China; 13599326589@139.com

³ China Energy Investment Corporation Science and Technology Research Institute Co., Ltd., Nanjing 210031, China; wangsheng9999@126.com

* Correspondence: heyuj@seu.edu.cn; Tel.: +86-138-5199-7665

Abstract: In recent years, the electrostatic-fabric integrated precipitator has been widely used, and the dust filtration performance of the core component filter bag is the most important factor affecting its dust removal efficiency. In this work, the dynamic dust removal performance of different types of filter media and different experimental conditions were studied on the filter media filtration performance test platform. The experimental study of the filtration performance of different types of filter media showed that the filtration performance stability of polyphenylene sulfide (PPS) filter media was better than that of polyimide (PI) and polytetrafluoroethylene (PTFE) filter media. Increasing the mass per unit area of the filter media had obvious advantages in the short term, and the impregnation process was beneficial to the filter performance of the filter media. Membrane-coated filter media had the best filtration performance, gradient filter media filtration performance was the second, followed by conventional filter media, ordinary blended, and ultrafine blended filter media. Studies with different experimental conditions found that the filtration efficiency increased with increasing resistance, was not significantly affected by changes in inlet dust concentration, but decreased with the increasing filtering velocity. This experimental results provided an important basis for the selection of filter bags for the electrostatic-fabric integrated precipitator project.

Keywords: electrostatic-fabric integrated precipitator; filter media; dynamic dust filtering characteristics; filtration performance; constant pressure ash cleaning



Citation: Chen, K.; Huang, Y.; Wang, S.; Zhu, Z.; Cheng, H. Experimental Research on Dynamic Filtering Characteristics of Filter Materials for Electrostatic-Fabric Integrated Precipitator. *Appl. Sci.* **2022**, *12*, 5824. <https://doi.org/10.3390/app12125824>

Academic Editor: Xiaohong Han

Received: 27 April 2022

Accepted: 4 June 2022

Published: 8 June 2022

Publisher's Note: MDPI stays neutral with regard to jurisdictional claims in published maps and institutional affiliations.



Copyright: © 2022 by the authors. Licensee MDPI, Basel, Switzerland. This article is an open access article distributed under the terms and conditions of the Creative Commons Attribution (CC BY) license (<https://creativecommons.org/licenses/by/4.0/>).

1. Introduction

At present, the situation of China's environmental problems is very serious, and air pollution, as one of the main representatives, is receiving more and more attention. Dust is the main factor of air pollution, especially as the most typical ones are PM_{2.5} and PM₁₀, which can cause a series of environmental problems such as haze, ozone layer destruction, the reduction of atmospheric visibility, and the greenhouse effect [1–5]. Coal-fired power plants are one of the important sources of dust emissions. The state has issued a series of policies and measures to strictly control the emission of air pollutants from coal-fired power plants. In 2015, the Ministry of Environmental Protection, the Development and Reform Commission, and the National Energy Administration jointly issued a notice on the "Comprehensive implementation of the work plan of ultra-low emission and energy-saving transformation of coal-fired power plants", and put forward the requirements of ultra-low emission and ensuring the energy-saving operation of environmental protection equipment for the pollutant control of coal-fired power plants [2,4]. In recent years, the electrostatic-fabric integrated precipitator and bag filter have achieved good results in the treatment of dust and particulate pollutants, but the filter bags on the market are various

and the effect is uneven, so the development of an excellent performance of filter bags has important significance [6–11].

Under the increasingly stringent national emission standards, the dust emission of coal-fired boilers has been controlled below 10 mg/Nm^3 , but the problem of fine dust emission has not been completely resolved. The removal of fine dust has become one of the mainstream directions of the current development of dust removal technology [5,12,13]. The main idea for removing fine dust is to combine fine dust into dust with a large particle size and then remove it. The methods mainly include electric coalescence, magnetic coagulation, steam phase change condensation, chemical agglomeration, etc. Among them, electric coagulation is the most commonly used technical means in coal-fired power plants [14–16]. As one of the mainstream dust removal technologies for coal-fired power plants in China, the electrostatic-fabric integrated precipitator is also facing technological innovation and upgrading under the background of ultra-low emissions in coal-fired power plants. The focus is to further improve the dust-removal performance of the electrostatic-fabric integrated precipitator while ensuring its low resistance operation [17–20].

The bag area is an important part of the electrostatic-fabric integrated precipitator, and the filter bag is the core component of the bag area [21]. The filtering performance of the filter bag directly affects the dust removal efficiency and running resistance of the dust collector [21–23]. At present, the commonly used basic filter materials are polyphenylene sulfide (PPS), polyimide (PI), polytetrafluoroethylene (PTFE), and so on [23–28]. In addition to the filter performance of the filter bag being affected by its material, factors such as weight, surface treatment process, and formula are also crucial. However, there is still very little research on filter bags. Therefore, it is of great significance to carry out comparative experiments on the filtering performance of filter materials with different materials, different weights, different surface treatment processes, and different formulations to guide the industrial application of filter bags.

2. Experimental Materials and Methods

2.1. Experimental Filter Material Properties

The experimental samples were all made by needle punching process, of which samples 1–7 were from Xiamen Zhongchuang Environmental Protection Technology Co., Ltd. (Xiamen, China) and samples 8–11 were from Lederer Technical Textiles Manufacturing (Shanghai) Co., Ltd. (Shanghai, China). The experimental samples are all of the types of filter media that are currently being used or will be used in practical projects. The basic parameters are shown in Table 1.

2.2. Experimental Method

The experiment uses the FEMA 1-AT (normal temperature type) filter material filtration performance test platform produced by FilT Eq, Germany (Figure 1), examines several filter materials of different materials and different processing techniques listed in Table 1, and measures their particle collection efficiency under different working conditions (constant pressure soot cleaning resistance, inlet dust concentration, filtering velocity, etc.). The preparation, testing, and calculation of the filter media samples for the experiment were based on the German standard VDI 3926-2004 and the Chinese national standard “Technical Requirements for Baghouse Dust Collectors” (GB/T 6719-2009). The test principle is: the dust was supplied through the precision spiral dust collector and introduced into the square vertical tube by the airflow, the dust concentration was 5 g/m^3 . The filter media sample was cut to the right size and clamped at the intersection of the horizontal and vertical tube. Under the suction of the vacuum pump, the dust-containing airflow passed through the tested filter media and the dust was trapped by the filter media. The filtering velocity was 2 m/min , the blowing pressure was 500 kPa , the pulse jet time was 50 ms , and the dust used for the test was Pural NF alumina dust produced in Germany with the particle size distribution as shown in Figure 2. The standard test conditions are shown in Table 2.

Table 1. Basic parameters of the experimental sample.

Sample	Class	Gram Weight (g/m ²)	Breathability (L/dm ² ·min)	Texture	Experimental Type
1	PPS fiber	544	148.68	PTFE	Different fiber material
2	PI fiber	560	192.48	PTFE	
3	PTFE fiber	730	126.44	PTFE	
4	PPS fiber	536	167.48	PPS	Different gram weight
5	PPS fiber	589	111.58	PPS	
6	PPS fiber by surface impregnation	540	178.84	PTFE	Different surface treatment process
7	(50%PPS + 50%PTFE) fiber	614	109.22	PTFE	
8	(70% common PPS + 30% superfine PPS) fiber	533	129.68	PTFE	Different mixed formulas
9	(Blended ultrafine) (70% common PPS + 30% superfine PPS) fiber	612	119.59	PTFE	
10	(gradient filter)				
11	PPS fiber coating a membrane	555	25.40	PTFE	Different mixed formulas
11	(50% PPS + 50% PTFE) fiber coating a membrane	621	13.86	PTFE	

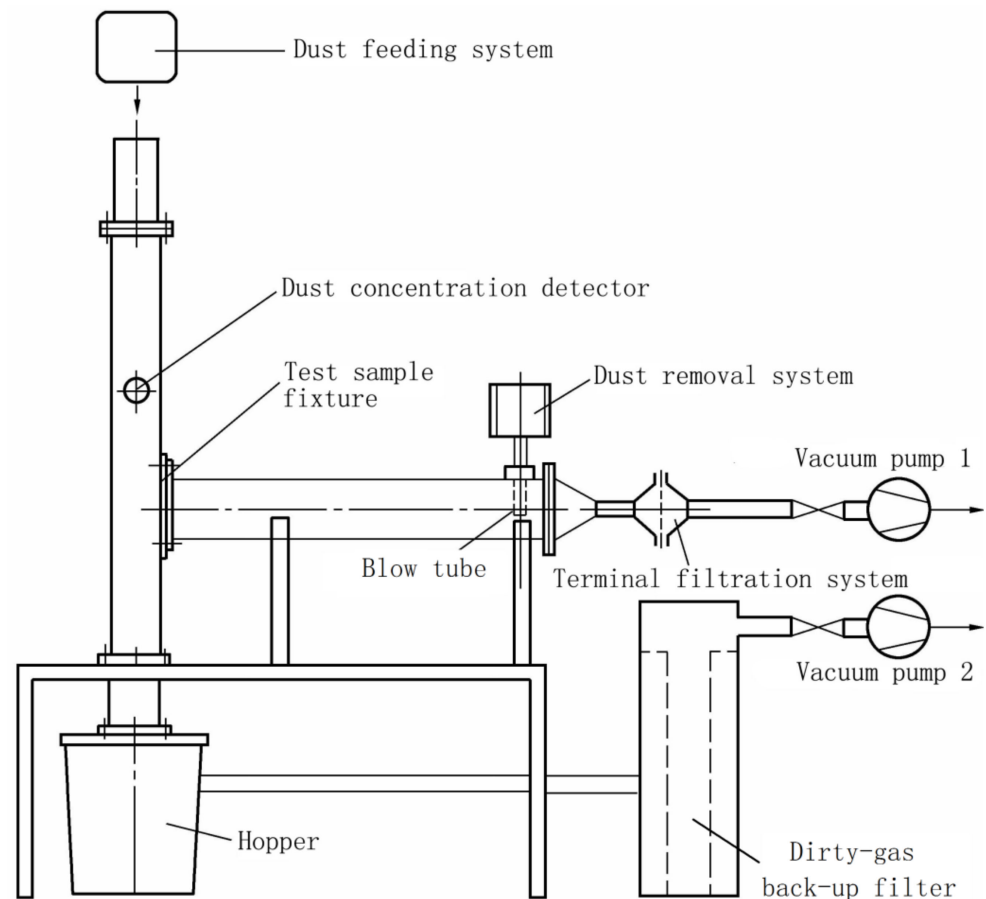


Figure 1. Filter material filtration performance test platform.

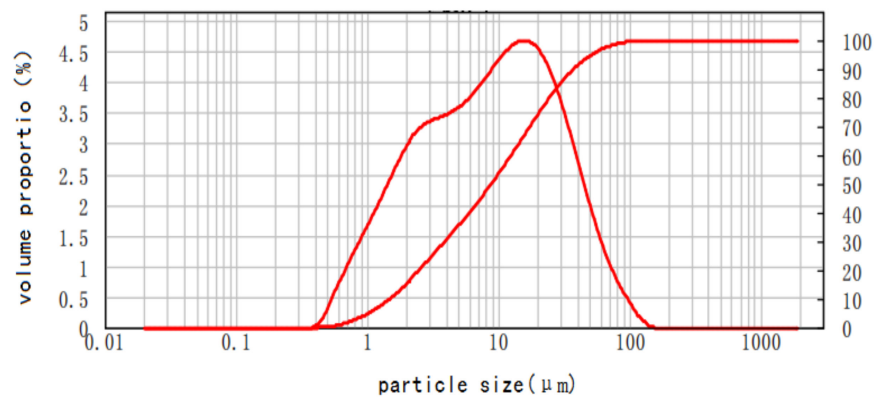


Figure 2. Standard dust particle size distribution.

Table 2. Standard test conditions.

Number	Parameter	Require	Remark
1	test dust	Aluminium oxide	Drying process: dry at 105–110 °C and place in the dryer for more than one hour
2	dust concentration	5 g/m ³	allowable deviation: ±7%
3	filtering velocity	2 m/min	allowable deviation: ±2%
4	injection pressure	5 bar	allowable deviation: ±3%
5	pulse jet time	50 ms	-
6	cleaning set-point pressure	1000 Pa	-
7	cleaning interval	5 s	ageing treatment

The test process was divided into four stages: cleaning, aging, stabilization, and measurement. The filter media was repeatedly filtered and back blown through these 4 stages. The performance of the filter media in the actual dust removal project was examined through the results of the 4 stages of operation in the system. The test steps were as follows:

- (1) Clean filter media sample filtration stage: Install the filter material sample on the filter material fixture, the diameter of the filter material sample was $\phi 150$ mm. When the pressure reached 1000 Pa, the pulse valve automatically opened for dust cleaning. The test time was recorded after 30 repetitions, the weight gain of the high-efficiency filter membrane was measured, and the exit dust concentration was calculated.
- (2) Aging treatment stage: Aging experiments were conducted on the experimental filter media, and back-blowing pulse cleaning was forced at 5 s intervals, with 10,000 repeated blows, and the process lasted for about 14 h. During the aging process, the pulse jet time was 50 ms, and the vacuum pump was kept working. The continuous blowing caused the filter media to repeat the process of tensioning and relaxing under the strong influence of changing airflow, which aggravated the aging of the filter media.
- (3) Stabilization treatment stage: in order to stabilize the filtration performance of the aged filter media samples, the experimental filter media was tested at a constant differential pressure of 1000 Pa for 10 cycles, according to (1).
- (4) The filtration performance of the filter media after stabilization: For the filter cloth stabilized as described above, a constant differential pressure stabilization test of 1000 Pa was performed 30 times according to (1). The test time was recorded, the weight gain of the high efficiency filter membrane was measured, and the outlet dust concentration was calculated.

The full process' instantaneous resistance values were recorded in the previous 4 tests and the dust removal efficiency was calculated. Using the mass method to calculate

the outlet dust concentration, the dust concentration and dust removal efficiency were calculated according to the following equation.

$$c = \frac{\Delta m}{Q \cdot t} \quad (1)$$

$$\eta = \frac{c_1 - c}{c_1} \times 100\% \quad (2)$$

where c is the outlet dust concentration (g/m^3), Δm is the weight gain of the high efficiency filter membrane (g), Q is the gas flow rate (m^3/h), t is the test time (h), η is the dust removal efficiency (%), and c_1 is the inlet dust concentration (g/m^3).

The surface microscopic morphology of the filter material was observed using a Phenom G2 benchtop SEM manufactured by FEI, the Netherlands. The sample was fixed to the nail sample stage using conductive adhesive, and the sample stage was held with tweezers and inserted vertically into the sample cup. Then, the sample cup was placed into the inspection chamber and the chamber door was closed to start observation and photography. The diameter of the observed sample was taken to be within 25 mm and the height within 30 mm, and the edge of the sample did not extend beyond the sample stage.

3. Results and Discussion

3.1. The Effect of Filter Material Properties on Filtration Efficiency

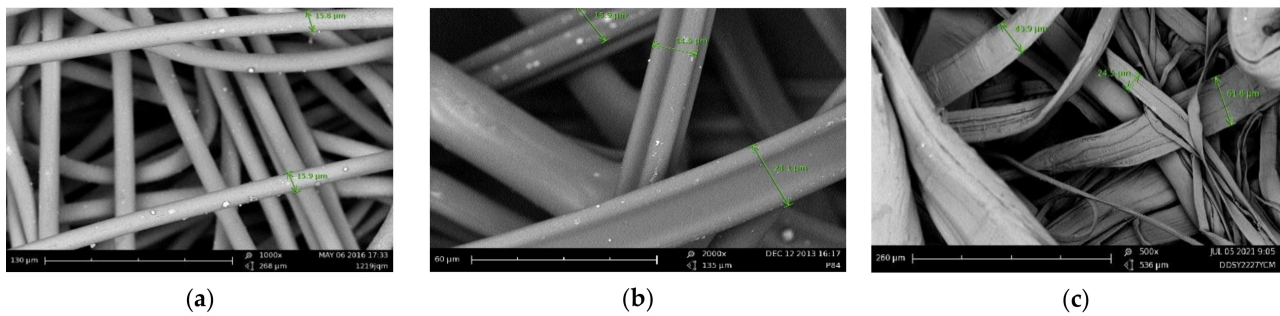
3.1.1. Comparison of the Filtration Efficiency of Different Materials of Filter Media

Under the standard test conditions in Table 2, the filter materials of PPS, PI, and PTFE (sample No. 1–3) were tested for comparisons of filtration efficiency. The experimental results were shown in Table 3. The surface microstructures of the filter materials of PPS, PI, and PTFE were shown in Figure 3.

It can be concluded from Table 3 that in the 30 cycles before aging, the PTFE filter material had the highest filtration efficiency, followed by the PPS filter material, and the PI fiber filter material had the lowest efficiency. After aging, the performance of the PPS filter material and PI filter material were significantly improved. Theoretically, the PI single fiber has a trilobal cross-section with a larger filtration surface area [29,30], and its filtration performance should be better than PPS and PTFE, but the results of this experiment were the opposite. In order to verify the filtration performance of the PI filter material, under standard test conditions, five PI filter cloths provided by different manufacturers were tested for the filtration performance. The test results show that the filtration efficiency of the PI sample cloth before aging was 99.9505–99.9575%, and the filtration efficiency after aging was 99.9874–99.9965%. The filtration efficiency of the filter cloth produced by different manufacturers was different, but the overall was still not as good as PPS. This might be because the filtration performance of the PI filter media was greatly affected by the manufacturing process. Although the PI fiber has a larger specific surface area, as the irregular fiber cross-section means that the fibers naturally curl, resulting in a strong holding force between the fibers and entanglement, the filtration performance itself is not necessarily better than PPS and PTFE filter media [31,32]. In addition, during the aging process of the PTFE filter material, due to the large amount of dust penetrating the filter material, the test system was blocked and the experiment was terminated, which shows that the PTFE filter media has a better filtration performance in the short term, but its filtration performance will be significantly reduced after long-term use. From the comparison of the experimental results of the three material filter materials, it is concluded that the PPS filter material has a high and stable filtration performance.

Table 3. Filtration efficiency of different material filtration materials.

	PPS (%)	PI (%)	PTFE (%)
Before aging	99.9790	99.9505	99.9824
After aging	99.9970	99.9921	/

**Figure 3.** Surface electron microscopy of (a) PPS, (b) PI, and (c) PTFE.

3.1.2. Comparison of the Filtration Efficiency of Filter Media with Different Grams

Under standard test conditions, the filtration efficiency of two kinds of PPS filter media (sample 4 and sample 5) with gram weights of $536 \text{ g}\cdot\text{m}^{-2}$ and $589 \text{ g}\cdot\text{m}^{-2}$ was experimentally compared. The experimental results were shown in Table 4.

Table 4. Filtration efficiency of different grams of PPS filter material.

	Pure PPS ($536 \text{ g}\cdot\text{m}^{-2}$) (%)	Pure PPS ($589 \text{ g}\cdot\text{m}^{-2}$) (%)
Before aging	99.9511	99.9878
After aging	99.9958	99.9948

It can be concluded from Table 4 that the filtration efficiency of the PPS filter material with a gram weight of $589 \text{ g}\cdot\text{m}^{-2}$ was significantly better than that of the PPS filter material with a gram weight of $536 \text{ g}\cdot\text{m}^{-2}$ in the 30 cycles before aging. However, after 30 cycles of aging, the filtration efficiency of the two was basically the same. It shows that a filter with a larger weight had a better filtration advantage in the short term, but after a period of use, there was no obvious advantage in the filtration efficiency [28,33,34]. For the same material and the same area of filter media, the grammage of the filter media was greater in density and surface area, which increased the chance of trapping dust particles. Therefore, for 30 cycles before aging, the filtering advantage of the filter media with high grammage was obvious, while for 30 cycles after aging, the filter media filtration mainly relied on the dust layer, so the filtration effect was not significantly affected by grammage.

3.1.3. Comparison of the Filtration Efficiency of Filter Media with Different Surface Treatments

The dipping process uses high-concentration emulsion to impregnate the needle felt as a whole, to achieve the effect of coating the surface of each fiber, which is equivalent to coating a layer of film on the surface of the fiber. The coating process is to use special equipment to coat the surface of the filter material, and then go through conventional processes such as the drying and heat setting. Both processes can improve the oxidation resistance, corrosion resistance, and temperature resistance of the filter material, and at the same time can improve the filtration accuracy of the filter material and prolong the service life of the filter material. After immersion treatment and coating treatment, the surface microstructure of the filter material was shown in Figure 4. It can be seen from Figure 3b that after the coating treatment, the surface of the filter material is coated with a film with different pore sizes.

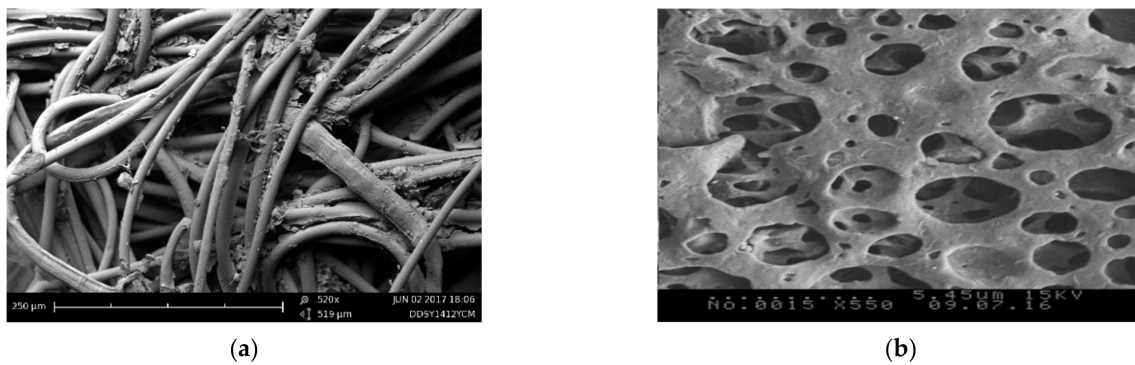


Figure 4. Filter material surface after immersion treatment (a) and coating treating (b).

Under standard test conditions, the PPS filter material (sample 1, sample 6) after immersion and the coating treatment was subjected to a comparative study of filtration efficiency. The experimental results were shown in Table 5. It can be seen from Table 5 that the filtration efficiency of the filter material before and after the aging of the two surface treatment processes was very high. However, compared to the coating treatment process, the filtration performance of the immersion treatment process was slightly superior. After the filter media was impregnated with PTFE, the PTFE emulsion entered the filter media and adhered to the surface of the fiber or filled the space between the fiber and the fiber, which inevitably reduced the internal pore size of the filter media and improved the filtration efficiency of the filter media for particulate matter. From the microscopic morphological analysis in Figure 4b, a microporous film was formed on the surface of the filter media after the coating treatment, which led to a reduction in porosity, thus affecting the filtration performance of the original filter media [33]. In addition, PTFE emulsion was not evenly distributed on the surface of the filter media, and the surface micropores were of different sizes, so the filtration accuracy of the coated filter media was greatly affected by the production process.

Table 5. Filtration efficiency of different surface treatment.

	Coating (%)	Dipping (%)
Before aging	99.9790	99.9960
After aging	99.9970	99.9976

3.1.4. Comparison of Filtration Efficiency of Filter Media with Different Formulations

Under standard test conditions, a comparative study of the filtration efficiency of PPS fibers (common, sample 1), 50% PPS + 50% PTFE (blending, sample 7), 70% conventional PPS + 30% ultra-fine PPS (blended ultra-fine, sample 8), 70% conventional PPS + 30% ultra-fine PPS (gradient filter media, sample 9), PPS fibers + laminate (common + membrane, sample 10), and 50% PPS + 50% PTFE + membrane (blended + membrane, sample 11) was carried out, and the experimental results are shown in Table 6.

Table 6. Filtration efficiency of different formula filters.

	Common Fiber (%)	Blending (%)	Blended Ultra-Fine (%)	Gradient Filter (%)	Common Fiber Coating a Membrane (%)	Blended Fiber Coating a Membrane (%)
Before aging	99.9790	99.9776	99.9702	99.9831	99.9998	99.9996
After aging	99.9970	99.9969	99.9911	99.9988	99.9997	99.9995

From Table 6, it can be concluded that among the six experimental filter media, whether it was conventional laminated filter media or blended laminated filter media, the laminated film played a major role in the filtration, which realized the transformation of deep filtration to surface filtration in the filtration mechanism, and the micro-particles did not easily enter the inner part of the filter media, with a high-efficiency filtration performance and filtration efficiency close to 100%. The gradient filter material was similar to the membrane-covered filter material in the structure, and formed the characteristics of the “surface filtration” mechanism; its filtration performance was close to the membrane-covered filter material [35,36]. Although the blended ultrafine fiber media was blended with ultra-fine ingredients, it did not form a gradient structure, so the filtration performance of blended microfiber filter media has no obvious advantages.

3.2. The Influence of Working Conditions on the Efficiency of Filter Media

Based on the 50% PPS + 50% PTFE blended filter material commonly used in the power industry (sample 7), the filter efficiency of the filter material under different working conditions was investigated.

3.2.1. Dust Filtration Efficiency of Filter Media under Different Constant Pressure Soot Cleaning Resistance

According to the standard test conditions in Table 2. When the constant pressure soot cleaning resistance was 800 Pa, 1000 Pa, and 1500 Pa, respectively, the filtration efficiency of sample 7 was determined, and the results were shown in Figures 5 and 6.

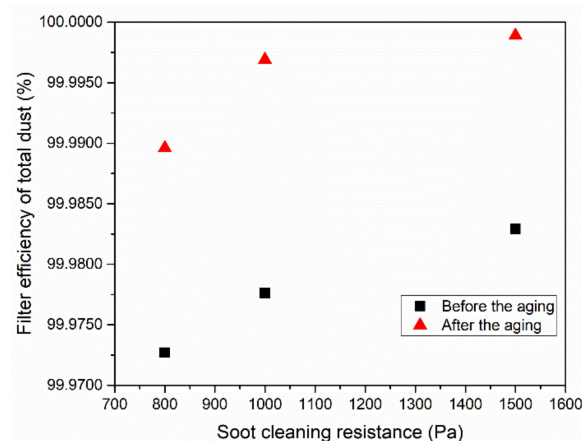


Figure 5. Filtration efficiency of filter media for total dust at different constant pressure soot cleaning resistances.

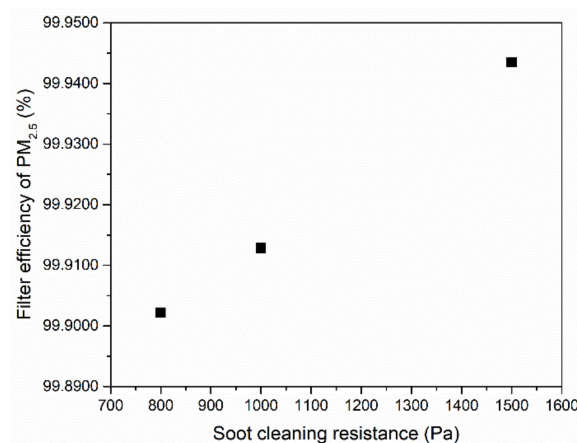


Figure 6. PM_{2.5} filtration efficiency of filter media at different constant pressure soot cleaning resistances.

It can be seen from Figures 5 and 6 that compared with before aging, the total dust filtration efficiency of the filter material after aging increased, and the total dust filtration efficiency and PM_{2.5} filtration efficiency both increased with the increase of the constant pressure soot cleaning resistance. This may be because the filter material mainly relies on the powder cake layer formed on the surface to filter dust. In addition, with the increase in the constant pressure soot cleaning resistance, the thicker the layer of powder cake is, and the higher the filtration efficiency.

3.2.2. Dust Filtration Efficiency of Filter Media at Different Inlet Concentrations

According to the standard test conditions in Table 4, the filtration efficiency of sample 7 was tested when the inlet dust concentration was 2 g·m⁻³, 3 g·m⁻³, and 5 g·m⁻³. The results were shown in Figures 7 and 8. It can be seen from Figures 7 and 8 that compared to before aging, the total dust filtration efficiency of the filter material after aging was improved, which is also the reason that a stable “powder layer” was formed on the surface of the filter material after aging [20,37]. Changing the inlet dust concentration, the filtering efficiency of the filter media on the total dust and PM_{2.5} was above 99.90%, and the difference between them was not obvious, which is consistent with the theory that the efficiency of bag dust removal is not affected by the inlet dust concentration.

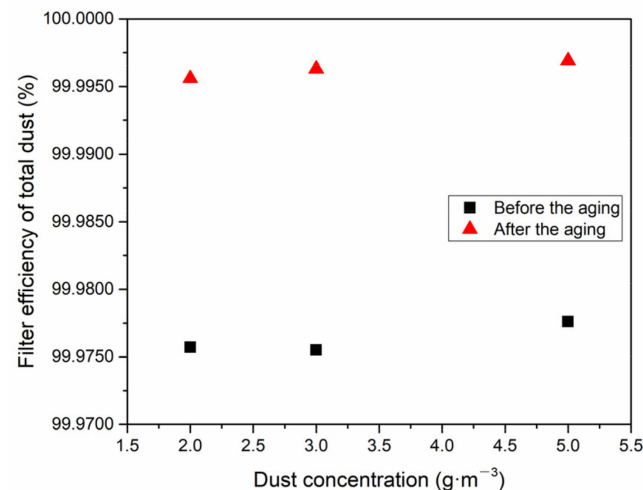


Figure 7. Filtration efficiency of filter media for total dust at different inlet dust concentrations.

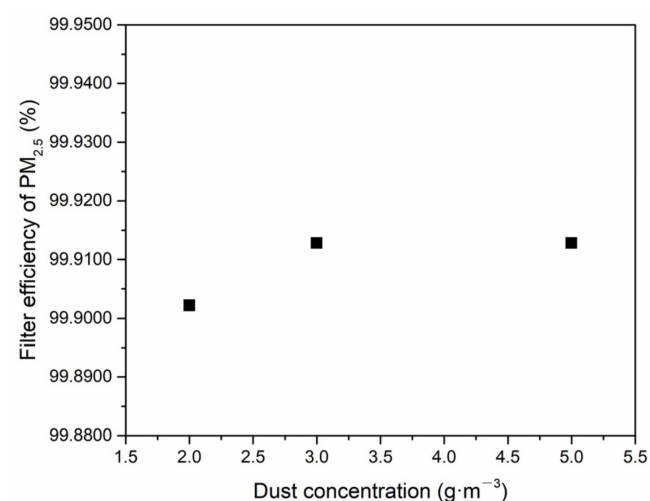


Figure 8. PM_{2.5} filtration efficiency of filter media at different inlet dust concentrations.

3.2.3. Dust Filtration Efficiency of Filter Media at Different Filtering Velocities

According to the standard test conditions in Table 4, the filtration efficiency of sample 7 was tested under the conditions of filtering velocities of $1.0 \text{ m}\cdot\text{min}^{-1}$, $1.5 \text{ m}\cdot\text{min}^{-1}$, $2.0 \text{ m}\cdot\text{min}^{-1}$, and $2.5 \text{ m}\cdot\text{min}^{-1}$. The results were shown in Figures 9 and 10. It can be seen from Figures 9 and 10 that the total dust filtration efficiency and $\text{PM}_{2.5}$ filtration efficiency were both higher than 99.9% at four different filtering velocities, and the total dust filtration efficiency of the filter material after aging was higher than before. The total dust filtration efficiency and $\text{PM}_{2.5}$ filtration efficiency both decreased with the increase of filtering velocity, and the decrease of the $\text{PM}_{2.5}$ filtration efficiency was slightly larger. The reason for the analysis was that as the filtering velocity increased, the airflow velocity per unit area through the filter layer increased, and the force driving the solid particles to penetrate the filter layer increased, which led to a decrease in the filtration efficiency. The equivalent diameter and unit mass of $\text{PM}_{2.5}$ fine particles were smaller, and the penetration rate was greater. Therefore, the filtration efficiency of $\text{PM}_{2.5}$ decreased slightly.

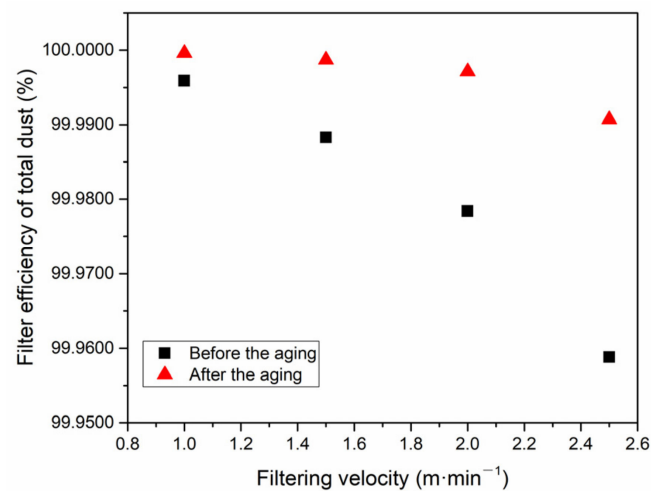


Figure 9. Filtration efficiency of filter media for total dust at different filtering velocities.

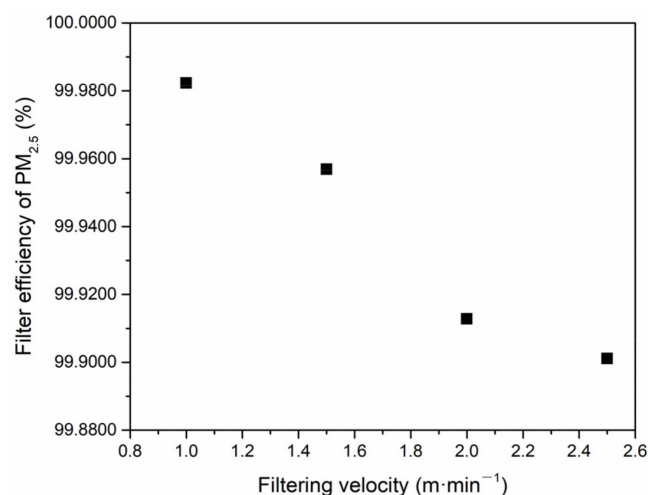


Figure 10. $\text{PM}_{2.5}$ filtration efficiency at different filtering velocities.

4. Conclusions and Outlook

In this work, tests on the filtration performance of different filter media were carried out, while the effect of different experimental conditions on the filtration performance was investigated. The following conclusions were drawn for this experimental condition.

- (1) Compared with PI and PTFE, PPS filter media had the highest filtration efficiency and the best filtration performance stability after a long period of operation.
- (2) Increasing the mass per unit area of the filter media could improve the filtration performance, but the advantages will become less and less in the long term.
- (3) The filtration effect of coated filter media was not as good as impregnation treatment because of the influence of the film formation process.
- (4) Membrane-coated filter media showed the highest filtration efficiency, gradient filter media filtration performance was the second, followed by conventional filter media, ordinary blended, and blended ultrafine filter media.
- (5) Changes in the experimental conditions had different effects on the dynamic dust filtration performance of the filter media. The filtration efficiency of the filter media increased with the increase of the constant pressure cleaning resistance. The filtration efficiency was slightly affected by the change in the inlet dust concentration, but decreased with the increase in filtering velocity.

The above test results and analysis provide a theoretical basis for the selection of filter media for engineering projects, especially for projects with ultra-low emission requirements, providing a range of options for high precision filtration media, such as membrane-coated filter media and gradient filter media. Unfortunately, due to the time factor and the limitations of the experimental conditions, the effect of different filter materials and experimental conditions on the dust removal performance was only studied at room temperature and a low concentration (inlet concentration of only 5 mg/m³). In fact, the actual working conditions of the filter media in the project are more complex, which has a certain influence on the use of the filter media, and its performance in actual engineering will be studied in depth in the next step.

Author Contributions: K.C.: conceptualization, writing—original draft preparation, data curation, methodology; Y.H.: writing—review and editing, funding acquisition, supervision, project administration; S.W.: validation, software; Z.Z.: data curation, investigation; H.C.: methodology. All authors have read and agreed to the published version of the manuscript.

Funding: This work was supported by the National Key R&D Program of China (2017YFB0603203).

Conflicts of Interest: The authors declare no conflict of interest.

References

1. Marcazzan, G.M.; Vaccaro, S.; Valli, G.; Vecchi, R. Characterisation of PM₁₀ and PM_{2.5} particulate matter in the ambient air of Milan (Italy). *Atmos. Environ.* **2001**, *35*, 4639–4650.
2. Sun, Y.L.; Zhuang, G.S.; Tang, A.H.; Wang, Y.; An, Z.S. Chemical characteristics of PM_{2.5} and PM₁₀ in haze-fog episodes in Beijing. *Environ. Sci. Technol.* **2006**, *40*, 3148–3155.
3. Choi, D.H.; Kang, D.H. Infiltration of Ambient PM_{2.5} through Building Envelope in Apartment Housing Units in Korea. *Aerosol Air Qual. Res.* **2017**, *17*, 598–607.
4. Xu, G.; Jiao, L.M.; Zhang, B.E.; Zhao, S.L.; Yuan, M.; Gu, Y.Y.; Liu, J.F.; Tang, X. Spatial and Temporal Variability of the PM_{2.5}/PM₁₀ Ratio in Wuhan, Central China. *Aerosol Air Qual. Res.* **2017**, *17*, 741–751. [[CrossRef](#)]
5. Marcazzan, G.M.; Ceriani, M.; Valli, G.; Vecchi, R. Source apportionment of PM₁₀ and PM_{2.5} in Milan (Italy) using receptor modelling. *Sci. Total Environ.* **2003**, *317*, 137–147.
6. Chen, K.X.; Huang, Y.J.; Wang, S.; Zhu, Z.P.; Lou, T.; Cheng, H.Q. Experimental study on graded capture performance of fine particles with electrostatic-fabric integrated precipitator. *Powder Technol.* **2022**, *402*, 117297. [[CrossRef](#)]
7. Heo, K.J.; Oh, H.J.; Eom, H.; Kim, Y.; Jung, J.H. High-performance bag filter with a super-hydrophobic microporous polytetrafluoroethylene layer fabricated by air-assisted electrospraying. *Sci. Total Environ.* **2021**, *783*, 147043. [[CrossRef](#)]
8. Feng, Z.B.; Long, Z.W.; Yu, T. Filtration characteristics of fibrous filter following an electrostatic precipitator. *J. Electrostat.* **2016**, *83*, 52–62. [[CrossRef](#)]
9. Dziubak, T. Performance characteristics of air intake pleated panel filters for internal combustion engines in a two-stage configuration. *Aerosol Sci. Technol.* **2018**, *52*, 1293–1307. [[CrossRef](#)]
10. Dziubak, T.; Bakała, L.; Dziubak, S.D.; Sybilski, K.; Tomaszewski, M. Experimental Research of Fibrous Materials for Two-Stage Filtration of the Intake Air of Internal Combustion Engines. *Materials* **2021**, *14*, 7149. [[CrossRef](#)]
11. Ji, X.Z.; Huang, J.Y.; Teng, L.; Li, S.H.; Li, X.; Cai, W.L.; Chen, Z.; Lai, Y.K. Advances in particulate matter filtration: Materials, performance, and application. *Green Energy Environ.* **2022**. [[CrossRef](#)]

12. Lee, K.-S.; Sohn, J.-R.; Park, Y.-O. Filtration performance characteristics of ceramic candle filter based on inlet structure of high-temperature and high-pressure dust collectors. *J. Ind. Eng. Chem.* **2015**, *21*, 101–110. [[CrossRef](#)]
13. Rodrigues, M.V.; Barrozo, M.A.S.; Gonçalves, J.A.S.; Coury, J.R. Effect of particle electrostatic charge on aerosol filtration by a fibrous filter. *Powder Technol.* **2017**, *313*, 323–331. [[CrossRef](#)]
14. Shim, J.; Joe, Y.-H.; Park, H.-S. Influence of air injection nozzles on filter cleaning performance of pulse-jet bag filter. *Powder Technol.* **2017**, *322*, 250–257. [[CrossRef](#)]
15. Dong, K.J.; Zou, R.P.; Yang, R.Y.; Yu, A.B.; Roach, G. DEM simulation of cake formation in sedimentation and filtration. *Miner. Eng.* **2009**, *22*, 921–930. [[CrossRef](#)]
16. Sobczyk, A.T.; Marchewicz, A.; Krupa, A.; Jaworek, A.; Czech, T.; ski, Ł.S.; Kluk, D.; Ottawa, A.; Charchalis, A. Enhancement of collection efficiency for fly ash particles (PM_{2.5}) by unipolar agglomerator in two-stage electrostatic precipitator. *Sep. Purif. Technol.* **2017**, *187*, 91–101.
17. Xu, Q.; Wang, G.; Xiang, C.; Cong, X.; Gai, X.; Zhang, S.; Zhang, M.; Zhang, H.; Luan, J. Preparation of a novel poly (ether ether ketone) nonwoven filter and its application in harsh conditions for dust removal. *Sep. Purif. Technol.* **2020**, *253*, 117555. [[CrossRef](#)]
18. Liu, X.C.; Shen, H.G.; Nie, X.L. Study on the Filtration Performance of the Baghouse Filters for Ultra-Low Emission as a Function of Filter Pore Size and Fiber Diameter. *Int. J. Environ. Res. Public Health* **2019**, *16*, 247. [[CrossRef](#)] [[PubMed](#)]
19. Yu, Y.; Xiong, S.; Huang, H.; Zhao, L.; Nie, K.; Chen, S.; Xu, J.; Yin, X.; Wang, H.; Wang, L. Fabrication and application of poly (phenylene sulfide) ultrafine fiber. *React. Funct. Polym.* **2020**, *150*, 104539. [[CrossRef](#)]
20. Xie, B.; Li, S.; Chu, W.; Liu, C.; Hu, S.; Jin, H.; Zhou, F. Improving filtration and pulse-jet cleaning performance of metal web filter media by coating with polytetrafluoroethylene microporous membrane. *Process Saf. Environ. Prot.* **2020**, *136*, 105–114. [[CrossRef](#)]
21. Nie, X.; Shen, H.; Wang, Y.; Zhou, L.; Liu, X.; Fang, M. Investigation of the pyrolysis behaviour of hybrid filter media for needle-punched nonwoven bag filters. *Appl. Therm. Eng.* **2017**, *113*, 705–713. [[CrossRef](#)]
22. Kim, J.-U.; Hwang, J.; Choi, H.-J.; Lee, M.-H. Effective filtration area of a pleated filter bag in a pulse-jet bag house. *Powder Technol.* **2017**, *311*, 522–527. [[CrossRef](#)]
23. Li, J.; Wu, D.; Wu, Q.; Luo, M.; Li, J. Design and performance evaluation of novel colliding pulse jet for dust filter cleaning. *Sep. Purif. Technol.* **2019**, *213*, 101–113. [[CrossRef](#)]
24. Huang, J.J.; Zhang, X.; Bai, L.L.; Yuan, S.G. Polyphenylene sulfide based anion exchange fiber: Synthesis, characterization and adsorption of Cr(VI). *J. Environ. Sci.* **2012**, *24*, 1433–1438. [[CrossRef](#)]
25. Stoeffler, K.; Andjelic, S.; Legros, N.; Roberge, J.; Schougaard, S.B. Polyphenylene sulfide (PPS) composites reinforced with recycled carbon fiber. *Compos. Sci. Technol.* **2013**, *84*, 65–71. [[CrossRef](#)]
26. Boudhan, R.; Joubert, A.; Durécu, S.; Gueraoui, K.; le Coq, L. Influence of air humidity on particle filtration performance of a pulse-jet bag filter. *J. Aerosol Sci.* **2019**, *130*, 1–9. [[CrossRef](#)]
27. Park, B.H.; Lee, M.-H.; Kim, S.B.; Jo, Y.M. Evaluation of the surface properties of PTFE foam coating filter media using XPS and contact angle measurements. *Appl. Surf. Sci.* **2011**, *257*, 3709–3716. [[CrossRef](#)]
28. Zhou, F.; Diao, Y.; Wang, R.; Yang, B.; Zhang, T. Experimental study on PM_{2.5} removal by magnetic polyimide loaded with cobalt ferrate. *Energy Built Environ.* **2020**, *1*, 404–409.
29. Jiang, S.H.; Uch, B.; Agarwal, S.; Greiner, A. Ultralight, Thermally Insulating, Compressible Polyimide Fiber Assembled Sponges. *ACS Appl. Mater. Interfaces* **2017**, *9*, 32308–32315. [[CrossRef](#)] [[PubMed](#)]
30. Gouzman, I.; Grossman, E.; Verker, R.; Atar, N.; Bolker, A.; Eliaz, N. Advances in Polyimide-Based Materials for Space Applications. *Adv. Mater.* **2019**, *31*, 1807738. [[CrossRef](#)]
31. Xie, F.; Wang, Y.; Zhuo, L.; Jia, F.; Ning, D.; Lu, Z. Electrospun Wrinkled Porous Polyimide Nanofiber-Based Filter via Thermally Induced Phase Separation for Efficient High-Temperature PMs Capture. *ACS Appl. Mater. Interfaces* **2020**, *12*, 56499–56508. [[CrossRef](#)] [[PubMed](#)]
32. Qiao, S.; Kang, S.; Zhu, J.; Wang, Y.; Yu, J.; Hu, Z. Facile strategy to prepare polyimide nanofiber assembled aerogel for effective airborne particles filtration. *J. Hazard Mater.* **2021**, *415*, 125739. [[CrossRef](#)] [[PubMed](#)]
33. Lyu, Q.; Ou, Q.S.; Chen, W.Q.; Wang, Y.J.; Chang, C.; Li, Y.J.; Che, D.F.; Pui, D.Y.H. Impacts of catalyst coating on the filtration performance of catalyzed wall-flow filters: From the viewpoint of microstructure. *Sep. Purif. Technol.* **2022**, *285*, 120417. [[CrossRef](#)]
34. Rozy, M.I.F.; Ito, K.; Une, K.; Fukasawa, T.; Ishigami, T.; Wada, M.; Fukui, K. A continuous-flow exposure method to determine degradation of polyphenylene sulfide non-woven bag-filter media by NO₂ gas at high temperature. *Adv. Powder Technol.* **2019**, *30*, 2881–2889. [[CrossRef](#)]
35. Saleem, M.; Khan, R.U.; Tahir, M.S.; Krammer, G. Experimental study of cake formation on heat treated and membrane coated needle felts in a pilot scale pulse jet bag filter using optical in-situ cake height measurement. *Powder Technol.* **2011**, *214*, 388–399. [[CrossRef](#)]
36. Saleem, M.; Krammer, G. Effect of filtration velocity and dust concentration on cake formation and filter operation in a pilot scale jet pulsed bag filter. *J. Hazard. Mater.* **2007**, *144*, 677–681. [[CrossRef](#)]
37. Dong, Y.; Gao, M.; Song, Z.; Qiu, W. Adsorption mechanism of As(III) on polytetrafluoroethylene particles of different size. *Environ. Pollut.* **2019**, *254*, 112950. [[CrossRef](#)] [[PubMed](#)]